SEISMIC VULNERABILITY OF HISTORICAL ARTIFACTS: EXPERIMENTAL TEST AND ANALYTICAL MODELING

A. Zamani Noori[1], C. Apostoliti[2], S. Marasco[3], A. Cardoni[4], M. Domaneschi[5], G.P. Cimellaro[6]

[1] *Postdoctoral research associate, Department of Structural, Geotechnical and Building Engineering, Politecnico di Torino, Italy, email: ali.zamani@polito.it*

[2] *PhD student, Department of Structural, Geotechnical and Building Engineering, Politecnico di Torino, Italy, email: carmelo.apostoliti@polito.it*

[3] *Postdoctoral research associate, Department of Structural, Geotechnical and Building Engineering, Politecnico di Torino, Italy, email: sebastiano.marasco@polito.it*

[4] *PhD student, Department of Structural, Geotechnical and Building Engineering, Politecnico di Torino, Italy, email: alessandro.cardoni@polito.it*

[5] *Assistant professor, Department of Structural, Geotechnical and Building Engineering, Politecnico di Torino, Italy, email: marco.domaneschi@polito.it*

[6] *Associate professor, Department of Structural, Geotechnical and Building Engineering, Politecnico di Torino, Italy, email: gianpaolo.cimellaro@polito.it*

Abstract

Historical artifacts represent a crucial aspect for societies and therefore it should be preserved from natural disasters (e.g. earthquakes). Artifacts such as statues are often made by fragile material, while present irregular shapes and different slenderness levels. Furthermore, a complete and accurate dynamic characterization can be achieved through the use of complex models. Indeed, friction is a crucial aspect which affects the behaviour of historical artefacts during dynamic excitations. Several studies investigated how friction is influenced from other parameters, such as artefact's geometry and motion characteristics. The paper investigates the relationship between the input velocity and dynamic friction coefficient through experimental dynamic test performed by shaking table. High and low velocity conditions are analyzed for free standing cylindrical concrete sample. Three input time histories with different maximum amplitude and predominant frequency are adopted to analyze various shaking conditions. The experimental campaign is aimed at determining the main factors which affect the dynamic friction while creating a consistent output dataset. Finite Element Models are implemented for modelling the dynamic behaviour of the artefact and then validate the obtained results.

1. Introduction

Historical artefacts play a crucial role for communities and therefore they need to be protected against hazardous events. In the last decades, seismic events (e.g. L'Aquila 2009, Emilia 2012, Centro Italia 2016), have damaged monuments and art goods highlighting their seismic vulnerability [1]. Currently, seismic safety is assessed by comparing artefact's response to the corresponding limit value. To accomplish this goal a detailed mathematical formulation of rigid body motion is required. The analytical first attempt to examine the dynamic behaviour of a rigid body was conducted by Housner [2] who investigated the case of body's rotation around one of the base corners. This simplified model was essentially based on the hypothesis of friction coefficient large enough to prevent any sliding. Ishiyama [3] classified the motion into six types based on slide, rotation and uplift combinations, taking into consideration the friction between the bottom surface of the object and its support. Overturning risk of rigid block under earthquake excitation ha been invetigated by Cimellaro and Domaneschi [4]. Beside the rigorous analytical formulation, Finite Element Method (FEM) is commonly adopted to determine the response of rigid bodies subjected to dynamic excitations [5]. However, FE analysis requires many assumptions regarding the mechanical properties of the materials and the boundary conditions to assume for the object and for its restraint. This last aspect plays a key role in the accuracy of the dynamic response assessment.

Many authors ([6], [7]) revealed the importance of some parameters, such as the strength and the friction coefficient between the artefact and its contact surface. Shenton [8] demonstrated that the motion of a free-standing rigid object on shaking plane depends not only on the object shape and the base acceleration, but also on the friction coefficient. Often, the friction between the art object and the support plane is assumed without reference to laboratory tests [9], causing a divergence in the expected results. A feasible calibration of the numerical model requires a large set of experimental results as stated from many researchers [10]. Monaco [11] adopted a unidirectional shaking table to determine the friction coefficient between the art object and the support. Different geometrical shapes and materials were investigated, while a wide variety of supporting surfaces were analysed.

Schimtz [12] focused on the experimental uncertainty associated with the instrumentation used in low dynamic friction coefficient measurements. A traditional pin-on-disk tribometer was employed to monitor the contact force vector which can be decomposed into friction force and normal force vectors. It was observed that a small misalignment of the force transducer axes relative to the surface may generate a not negligible relative error in friction coefficient estimation. Another important parameter to be accounted in the dynamic coefficient estimation is the relative moving velocity of the two contact surfaces. Shih and Sung [13] developed a smart measuring device to measure the kinetic friction coefficient based on the Arduino boards, motion sensor, and SD module. Accelerations and displacements were recorded with different angles and lubrication conditions, while the dynamic coefficient was calculated through physical mathematical model. The dynamic friction coefficient tends to decrease first and then to increase as the moving speed of the test object increases under the medium and non-lubricated conditions.

Despite the raising prominence in experimental tests, the available data still lack, and therefore the calibration of numerical models is an open issue. Furthermore, a more effective method capable of accurately identifying a mathematical formulation of the dynamic friction is required. This paper presents the results of a research program containing the experimental determination of the friction coefficient between free standing cylindrical concrete sample and a sanding paper support. The dynamic tests have been performed using a unidirectional shaking table, while high and low velocity conditions have been investigated.

2. Experimental evaluation of the dynamic friction coefficient

A special set-up of dynamic test has been developed based on the original idea of Aydan [14]. The experimental campaign consists of a dynamic application of a horizontal load on the specimen though a

unidirectional shaking table. Tests have been performed on cylindrical specimen of concrete on sanding paper supporting surface.

2.1 Experimental setup

The footprint specimen has a radius of 11 cm and a height of 8,5 cm, with a mass of 8 kg. The specimen of concrete is supported on a layer of sanding paper fixed on the horizontal plan of the shaking table. A load cell is connected to the specimen through a horizontal hollow steel profile which is welded on a vertical rigid steel element (Fig. 1). The horizontal profile is directly connected on the top of the specimen, while the load cell is screwed on the horizontal steel element. The ABS specimen-load cell connection elements have been obtained through 3D printing.
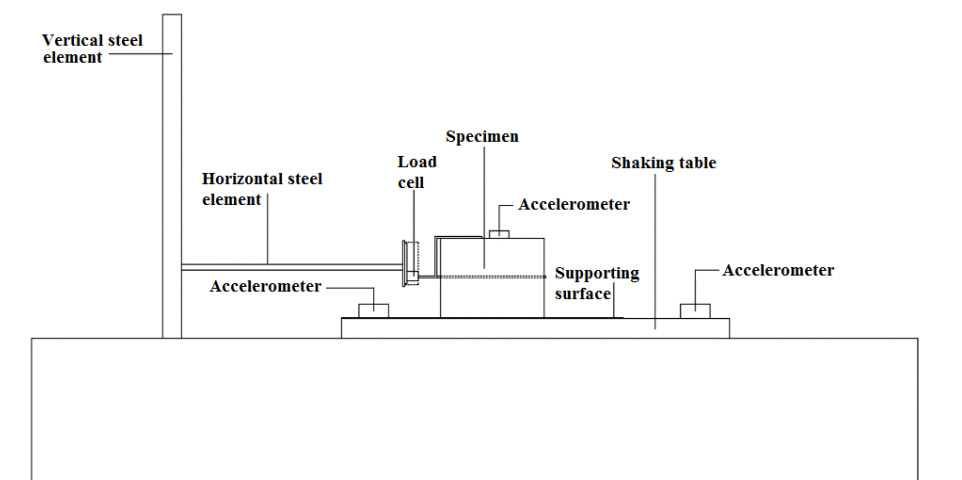

Fig. 1 – Scheme of test setup

The relative movement between the supporting surface and the specimen is ensured by the horizontal load provided by the fixed steel element system as result of reaction to the relative displacement due to the shaking table. A pair of accelerometers is employed to record the shaking table acceleration and the specimen top's surface. Fig. 2a shows an image of the test apparatus adopted to assess the dynamic friction coefficient.

Fig. 2 – Shaking table test setup

The shaking table consists of steel profiles, whereas the upper platform, where specimens can be fixed, is made of aluminium [15]. Two parallel tracks are located side by side and connected through transversal rectangular sections (Fig. 3). Tracks' profiles are 3 meters long and the section's size is 40x100x4 mm. Upon the steel profiles there are aluminium guides allowing the motion, along the longitudinal direction, of sliders that support two 600x500x10 mm aluminium platforms. Each track has its own platform, which is moved by a linear electric actuator anchored under it. Type and section of the steel profiles are the same of the bottom ones, while the length is shorter (600 mm). The linear electric actuators adopted are manufactured by the company LinMot and each is made of a stator, a slider and a motor. The longitudinal ones have a slider's length of 800 mm and a maximal stroke of 510 mm, whereas the transversal ones have a slider's length of 500 mm and a maximal stroke of 330 mm. The power supply, the two transformers and the four drivers to control the motors are provided by LinMot. The drivers are fundamental for the tuning of the motors (i.e. the initial configuration of all the control parameters) to have a response coherent with the input data. This operation is done through the software LinMot-Talk that is also used to switch on the actuators and to bring them in the home position. The software used for the activation and control of the shaking table is LabView. The seismic input is sent to the shaking table through a myRIO device manufactured by National Instruments. This device is physically connected to the motors' drivers and also to an accelerometer, which is located on the platform and allows catching the actual response of the system.
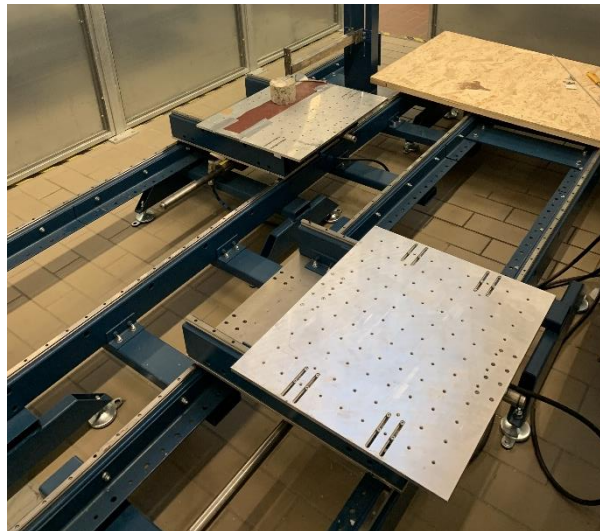

Fig. 3 – Shaking table

The accelerometers and the load cell are connected each other to synchronize the output value. The sampling frequency of load cells and accelerometer is 10 Hz, while a dynamic sinusoidal input with frequency of 83 Hz is adopted.

2.2 Experimental methodology and calculation method

The LabView code is used to set the input and output sampling rates to generate a sinusoidal seismic signal or to load a real one. The shaking table test consists in the assessment of the shear force acting on the surface between concrete sample and sanding paper through the load cell. Comparing accelerations recorded on the shaking table surface (a_g), and that one derived from the load cell (a_s), the friction acceleration (a_f) can be computed (Eq. (1)).

$$a_f = a_g - a_s$$

(1)

Therefore, the dynamic friction coefficient (μ_d) is obtained as given in Eq. (2):

4

$$\mu_d = \frac{a_f}{g} \tag{2}$$

A Matlab code is implemented to calculate the displacement and velocity in each time step of the test, allowing to obtain the relationship between the dynamic coefficient and the input velocity.

2.3 Valuation of measuring errors

The experimental evaluation of dynamic friction coefficient is affected by measurement uncertainties which affect the goodness of the results. Commonly, these errors arise from incorrect specimen set-up and inaccurate calibration of the measuring device. Among the others, the misalignment between the measuring axes (*X,Y* in Fig. 4) and the normal and tangential ones (*N,T* in Fig. 4) causes an error in the assessment of the normal and friction forces.
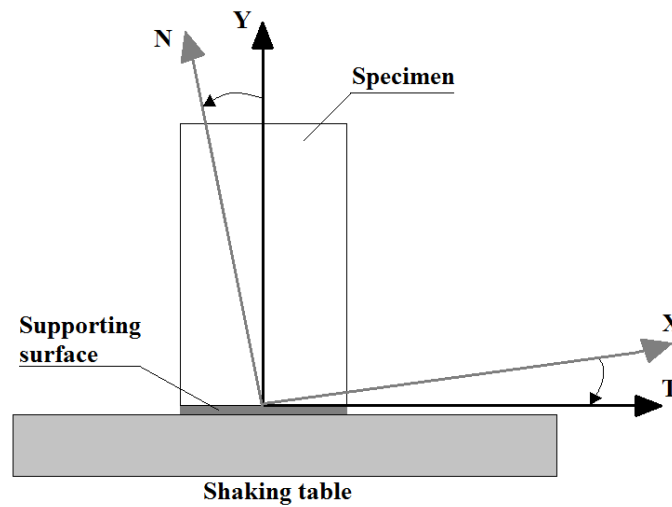

Fig. 4 – Misalignment errors

The acceleration values recorded on *X* and *Y* axes are the components of gravity acceleration due to the accelerometer's misalignment angles. Therefore, the dynamic friction coefficient measure is affected by an error *E* as given in Eq. (3):

$$E = \frac{a_f - \sqrt{a_{fx}^2 + a_{fy}^2}}{a_f} \tag{3}$$

where a_{fx} and a_{fy} are the friction acceleration components in *X* and *Y* directions, respectively. Thus, the dynamic friction coefficient μ_d can be assessed as given in Eq. (4).

$$\mu_d = \mu_{dm} \pm E \tag{4}$$

where μ_{dm} identifies the mean calculated value of the dynamic friction coefficient.

3. Experimental results

Three different dynamic inputs have been adopted to simulate different motion conditions. The first input motion is representative of a constant frequency signal and progressively decreasing amplitude (Fig. 5.a), while the second dynamic inputs refers to a real time history recorded during the Central Italy earthquake (2016/10/30, Fig. 5.b). The third motion refers to a sweep signal with constant amplitude (Fig. 5.c). The related accelerations (a_s) measured by the accelerometers installed on the shaking table are also illustrated in Fig. 6.
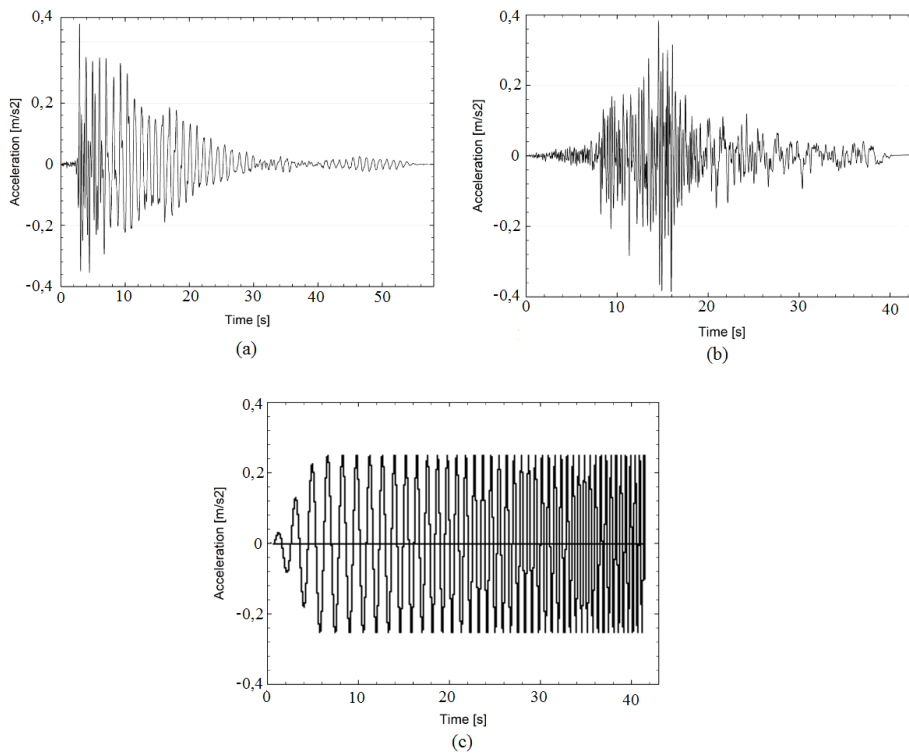
5

Fig. 5 – First (a), second (b), and third (c) input motion
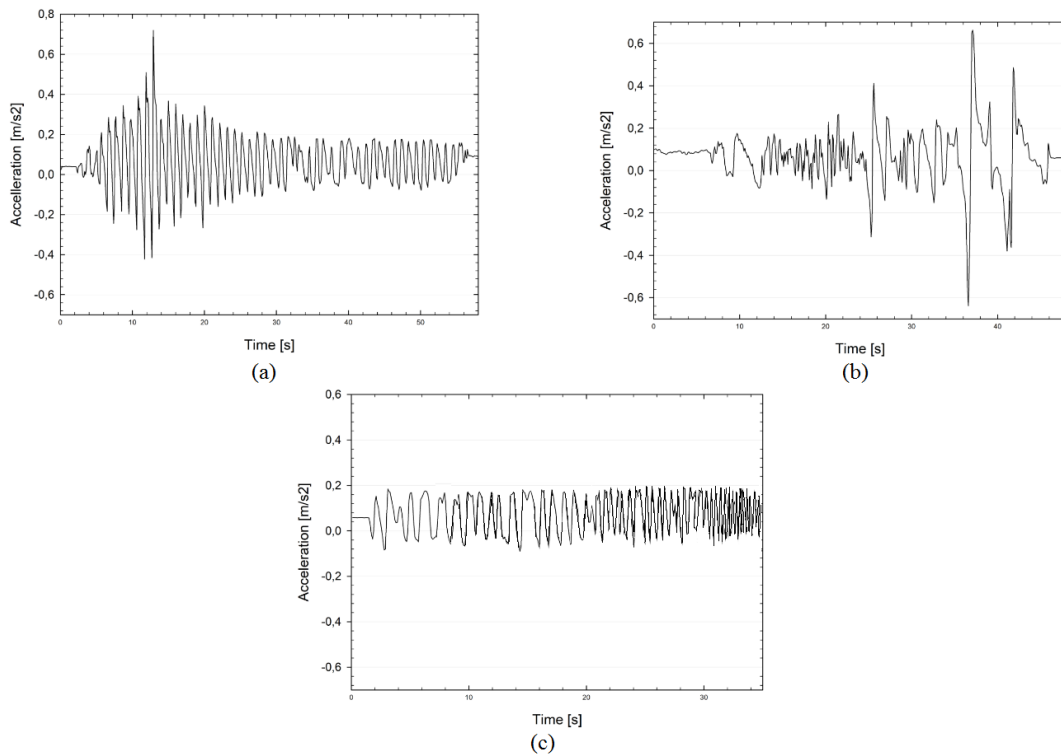

Fig. 6 - First (a), second (b), and third (c) measured acceleration on the specimen

6

Dynamic friction coefficient is assessed at each time step in order to identify the dependence on the motion velocity. Fig. 7 depicts the dynamic friction variation with the motion velocity.
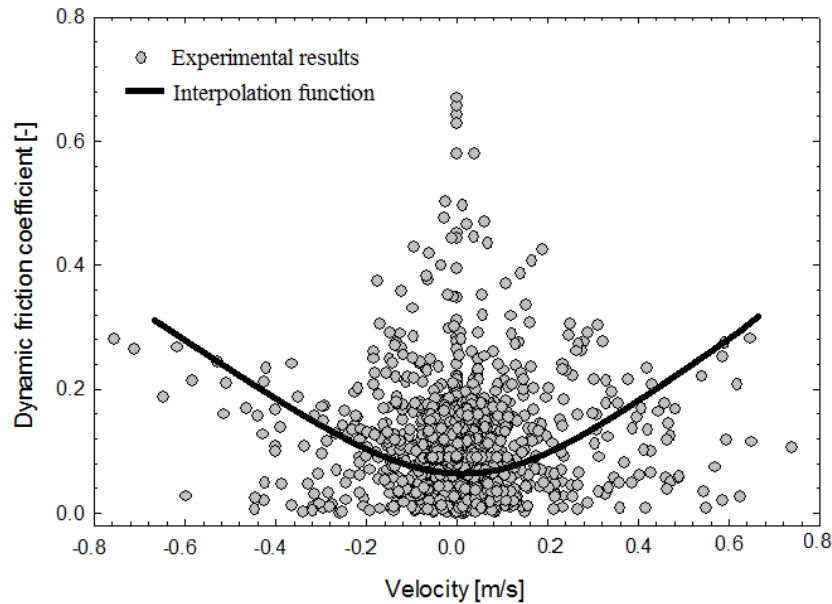

Fig. 7 – Relation between dynamic friction coefficient and motion velocity

The result of test confirms that the dynamic friction coefficient depends on the velocity of the excitation. In particular, the action of an earthquake induces positive and negative velocity, which means that the rigid sample passes continuously trough static and dynamic conditions. For dynamic conditions (-0,1<v<0,1 m/s), the dynamic friction coefficient monotonically increases. In case of quasi static conditions, the friction coefficient tends to correspond to the static friction coefficient. The mathematical relationship between motion velocity and friction coefficient is approximated by a polynomial equation given in Eq. (5).

$$\mu = 0.29 \cdot v^2 - 0.04 \cdot v + 0.11 \tag{5}$$

where v represents the motion velocity. Eq. (5) demonstrates that for quasi static conditions the friction coefficient tends to be equal to the static one (μ=0.11).

4. Numerical method

The reliability of the numerical analysis depends on different assumptions such as material behavior and geometric nonlinearity of the contact surfaces. To verify the experimental tests, a 3D Finite Element (FE) model has been created using SAP2000 by introducing the friction coefficient at different velocities. This software is capable to model the geometric nonlinearity of the contact surfaces. The specimen has been modelled with 8 nodes solid elements and the material strength class has been defined as f'_c=25 MPa (class C20/25 according to NTC2018). Fixed restraints have been assigned at the top surface and side face perpendicular to the direction of motion in order to model the specimen's boundary condition (Fig. 8).

To consider the effect of friction, Friction-Pendulum Isolator elements have been used to model the contact surface (Fig. 8). This element is able to model combination of different conditions varying from at-rest to slide, or from uplift to slam-down for the cases of friction and rocking, respectively. The pendulum radius of the slipping surface was set to zero to consider the flat surface friction. The element models the

7

coupled biaxial friction at contact surface considering the post-slip stiffness. In particular, along horizontal directions, two different friction coefficients have been defined to take into account the slow and fast velocity conditions, while in vertical direction only the vertical stiffness has been defined for model stability. The friction forces are proportional to both external normal force and friction coefficient. The axial force (P) is modeled with a compression-only gap element that does not carry the tension force in the case of uplift and it is given by:
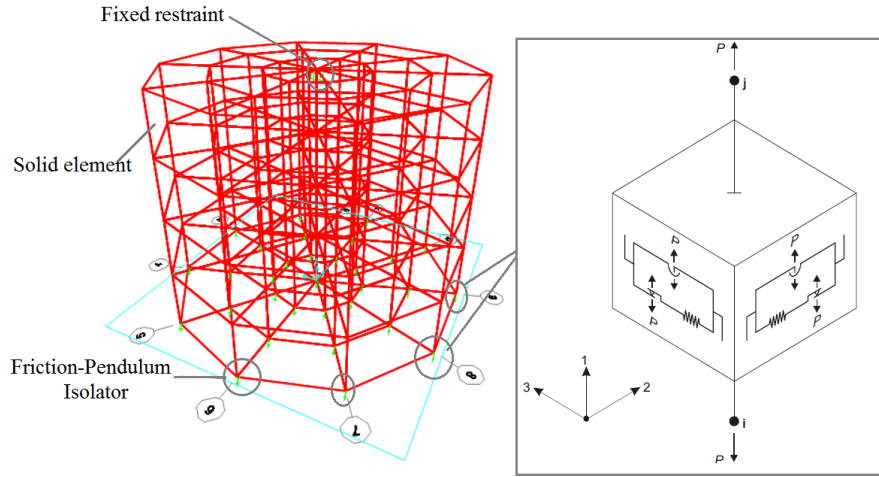

Fig. 8 – Finite element solid model using the Friction-Pendulum Isolator element

$$P = \begin{cases} K_z d_z & \text{if } d_z < 0 \\ 0 & \text{otherwise} \end{cases} \tag{5}$$

where the K_z is the vertical stiffness in negative axial direction (-Z) and d_z is the vertical displacement of the rigid body base at the contact surface. K_z has been set to some large value in order to consider the rigidity of the contact surface. The nonlinear behaviour is considered for each shear (friction) degree of freedom in x and y directions. The friction force-deformation relationship is given by:

$$f_x = -P\mu_x z_x$$
$$f_y = -P\mu_y z_y \tag{6}$$

where f_x and f_y are the friction forces in x and y directions, μ_x and μ_y are velocity-dependent friction coefficients to consider the different coefficients of friction for fast velocity versus slow velocity conditions, and z_x and z_y are internal hysteretic variables. In order to accurately model the problem, the fast and slow friction coefficients have been considered as a function of velocity. The initial values of z_x and z_y are zero and they evolve according to following differential Eq. (7):

$$\begin{Bmatrix} \dot{z}_x \\ \dot{z}_y \end{Bmatrix} = \begin{pmatrix} 1 - a_x z_x^2 & -a_y z_x z_y \\ -a_x z_x z_y & 1 - a_y z_y^2 \end{pmatrix} \begin{Bmatrix} \dfrac{K_x}{P\mu_x} \dot{d}_x \\ \dfrac{K_y}{P\mu_y} \dot{d}_y \end{Bmatrix} \quad \text{for } \sqrt{z_x^2 + z_y^2} \leq 1 \tag{7}$$

8

where K_x and K_y are the elastic shear stiffness constants in the absence of sliding, and a_x and a_y are binaries parameters deepening on velocity in x and y direction:

$$a_x = \begin{cases} 1 & \text{if } \dot{d}_x z_x > 0 \\ 0 & \text{otherwise} \end{cases}, \, a_y = \begin{cases} 1 & \text{if } \dot{d}_y z_y > 0 \\ 0 & \text{otherwise} \end{cases} \tag{8}$$

A high value of the pre-slip stiffness property in the horizontal direction has been used. This value does not affect the dynamics of the model, but only it is used to avoid ill-conditioned problem. This value has been selected as one order magnitude less than the value defined for the effective linear vertical stiffness. In addition, post slip stiffness has been set to values obtained from experimental tests to verify the results for different velocity conditions.

4.1 Numerical results

The results of the experimental tests have been compared with the FE model. Three different dynamic tests have been performed and the response of the model at the top surface (fixed restraint point in Fig. 8) has been assessed in terms of acceleration. The friction coefficients at different velocity condition (slow and fast) have been varied until the response of the FE model corresponds to the force recorded by the load cell in experimental tests. The final value used for slow and fast friction velocities are 0.23 and 0.4, respectively. Fig. 9 shows the results obtained from numerical modelling and experimental tests. Results show that the dynamic friction first decreases and then it increases proportionally to the velocity (Fig. 7). Results show a good agreement which confirms the reliability of the experimental tests to evaluate the dynamic friction coefficient. However, for the third input motions (Fig 5.c, and Fig. 6.c), the result is more compatible with that one obtained from experimental test.
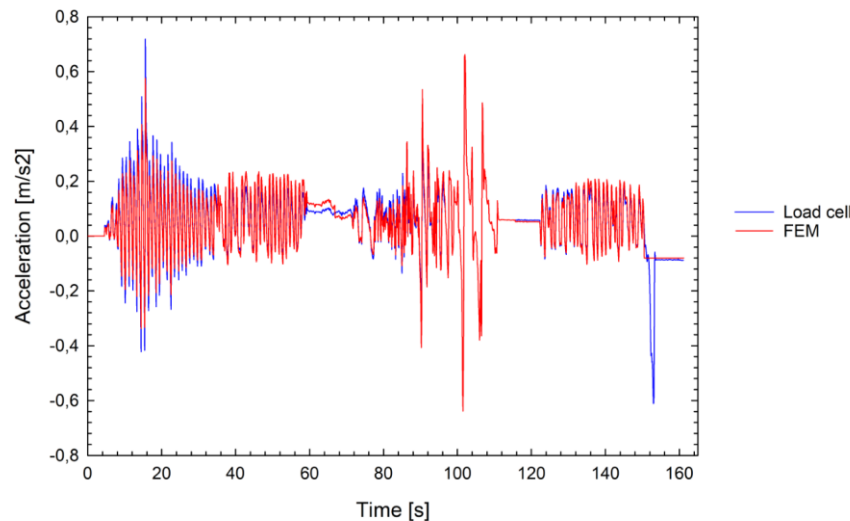

Fig. 9 - Comparison between FEM model and experimental test

5. Conclusions

In this paper the dynamic friction coefficient under different velocity conditions was investigated. Experimental tests were performed using a shaking table developing a new setup capable of measuring the friction coefficients at low and fast velocity conditions. A mathematical formulation between velocity and dynamic friction coefficient was extrapolated by a preliminary test on a benchmark specimen. Further, the

9

results were verified by a numerical finite element model taking into account the dynamic sliding effect. Results reveal that the dynamic friction coefficient is strongly affected by the input signal frequency. The dynamic friction coefficient presents a tendency to decrease first and then to increase proportionally to the velocity, while for quasi static conditions it remains almost equal to static friction coefficient. Test results demonstrated that the proposed setup configuration, which is low in price and easy to assemble, can be used to measure the dynamic friction coefficient of specimens under various conditions. Future work will focus to study the dynamic coefficient taking into account the influence of normal force, specimen different material and geometrical configurations.

6. Acknowledgements

7. Copyrights

8. References

[1] Parisi F, Augenti N (2013): Earthquake damages to cultural heritage constructions and simplified assessment of artworks. *Engineering Failure Analysis*, **34**, 735-760.

[2] Housner GW, Hudson DE (1965): *Applied Machanics Dynamics*.

[3] Ishiyama Y (1975): The theory of optimum currency areas: a survey. *Staff Papers*, **22**(2), 344-383.

[4] Cimellaro GP, Domaneschi M, Qu B (2020): Overturning risk of furniture in earthquake-affected areas. *Journal of Vibration and Control*, **26**(5-6), 362-374.

[5] Konstantinidis D, Makris N (2005): Seismic response analysis of multidrum classical columns. *Earthquake engineering & structural dynamics*, **34**(10), 1243-1270.

[6] Viti S, Tanganelli M, D'intinosante V, Baglione M (2019): Effects of soil characterization on the seismic input. *Journal of Earthquake Engineering*, **23**(3), 487-511.

[7] Spanos PD, Koh A-S (1984): Rocking of rigid blocks due to harmonic shaking. *Journal of Engineering Mechanics*, **110**(11), 1627-1642.

[8] Shenton III HW (1996): Criteria for initiation of slide, rock, and slide-rock rigid-body modes. *Journal of Engineering Mechanics*, **122**(7), 690-693.

[9] Sinopoli A (1987): Dynamics and impact in a system with unilateral constraints the relevance of dry friction. *Meccanica*, **22**(4), 210-215.

[10] Baggio S, Berto L, Favaretto T, Saetta A, Vitaliani R (2015): Seismic isolation technique of marble sculptures at the Accademia Gallery in Florence: numerical calibration and simulation modelling. *Bulletin of Earthquake Engineering*, **13**(9), 2719-2744.

[11] Monaco M, Guadagnuolo M, Gesualdo A (2014): The role of friction in the seismic risk mitigation of freestanding art objects. *Natural hazards*, **73**(2), 389-402.

[12] Schmitz TL, Action JE, Ziegert a, John C, Sawyer WG (2005): The difficulty of measuring low friction: uncertainty analysis for friction coefficient measurements. *J. Trib.*, **127**(3), 673-678.

[13] Shih M-H, Sung W-P (2019): Developing Smart Measurement Device to Measure Kinetic Friction Coefficients of Bi-Tilt Isolator. *Advances in Civil Engineering*, **2019**.

[14] Aydan Ö (2019): Some considerations on the static and dynamic shear testing on rock discontinuities. *2019 Rock Dynamics Summit: Proceedings of the 2019 Rock Dynamics Summit (RDS 2019), May 7-11, 2019, Okinawa, Japan*, 201.

[15] Cimellaro GP, Domaneschi M (2018): Development of Dynamic Laboratory Platform for Earthquake Engineering Courses. *Journal of Professional Issues in Engineering Education and Practice*, **144**(4), 05018015.